Journal of Sound and Vibration (2000) **235**(5), 847–861
doi:10.1006/jsvi.2000.2950, available online at http://www.idealibrary.com on IDEAL®

VIBRATION OF LINEAR GUIDEWAY TYPE RECIRCULATING LINEAR BALL BEARINGS

HIROYUKI OHTA

Department of Mechanical Engineering, Nagaoka University of Technology, Kamitomioka, Nagaoka, Niigata, Japan

AND

EIJI HAYASHI

Precision Machinery & Parts Technology Center, NSK Ltd. Toriba, Maebashi, Gunma, Japan

(*Received* 24 *November* 1998, *and in final form* 15 *March* 2000)

The vibration of linear guideway type (LGT) recirculating linear ball bearing driven at a constant linear velocity was studied. The measurement results of the vibration showed that the overall levels of vibratory velocity of the LGT recirculating linear ball bearings change with the measurement point of the vibration, and they are affected by linear velocity and preload. We also observed the main peaks in the vibration spectra of the LGT recirculating linear ball bearing itself. The main peaks were analyzed using the modal analysis, the frequency expressions for the rigid-body natural vibrations of the carriage and the finite element method. As a result, it was made clear that the main peaks are caused by the lower rolling, the yawing, the pitching, the vertical, the higher rolling, the first flexural, the second flexural and the third flexural natural vibrations of the carriage.

1. INTRODUCTION

Linear motion rolling bearings have many advantages compared with conventional sliding guides such as flat ways and V-ways [1]. For instance, abrasion of linear motion rolling bearings is less than that of sliding guides, and they have no stick slip. Therefore, linear motion rolling bearings have been widely used instead of sliding guides in machining centers, lathes, grinding machines, robots, precision X–Y tables, measuring systems and transport systems [2]. In recent years, the speed of machines using linear motion rolling bearings has increased, therefore the vibration of linear motion rolling bearings has added to the serious problem of vibration of these machines. Kasai *et al.* [3, 4] found out that carriages of the preloaded linear guideway type (LGT) recirculating linear ball bearings were moved periodically with the ball passing frequency due to ball circulation. This motion has been called "ball passing vibration". They also pointed out that the ball passing vibration was reduced by using a carriage with crowned raceways. Moreover, they showed the frequency expression of the ball passing vibration. Shimizu [5] observed the ball passing vibration and the harmonics of it in the table using the LGT recirculating linear ball bearings. Ye *et al.* [6] carried out a modal analysis for carriages of LGT recirculating linear ball bearings under stationary conditions and pointed out the existence of the rigid-body natural vibrations of the carriage. Shimo [7] measured damping characteristics of linear

0022-460X/00/350847 + 15 $35.00/0

motion rolling bearings. He pointed out that the linear roller bearings had substantially shorter decay time than the linear ball bearings. Schneider [8] developed a theory for the natural vibrations of an LGT recirculating linear ball bearing having a 45° contact angle. In the vibratory model of his theory, mass and inertia of moment of a carriage having additional mass were considered and normal springs due to elastic contacts between each ball and raceway were replaced by four vertical springs and four horizontal springs. Unfortunately, he did not compare the result obtained by his theory and vibration of LGT recirculating linear ball bearings in operation. Grunau and Giese [9] measured the vibration characteristics of a machine tool table using LGT recirculating linear ball bearings. Recently, one [10] of the authors measured the sound of an LGT recirculating linear ball bearing itself operated at a constant linear velocity. Moreover, he derived the frequency expressions for the rigid-body natural vibrations of an LGT recirculating ball bearing having an arbitrary contact angle, and proved that the main peaks in the sound spectra are caused by the lower rolling natural vibration of the carriage, the pitching natural vibration of the carriage and the vertical natural vibration of the carriage.

In this study, as a first step toward the understanding of the vibration of linear motion rolling bearings, the vibration of an LGT recirculating linear ball bearing itself operated at a constant linear velocity is explained. In this paper, we first discuss the measuring method of the vibration by using the drive unit for measurement of sound and vibration of linear motion rolling bearings [11]. Second, we measure the vibration characteristics such as overall level of vibratory velocity and vibration spectra of the LGT recirculating linear ball bearing at a constant linear velocity. Third, to explain the main peaks which appeared in the vibration spectra, we examine the modes of the carriage and carry out the natural vibration analysis of the LGT recirculating linear ball bearing. Finally, we discuss the relationship between the main peak and the natural vibration of the carriage.

2. EXPERIMENTS

2.1. TEST LINEAR BEARINGS

The test linear bearings used in the vibration measurement are the LGT recirculating linear ball bearings shown in Figure 1. One test linear bearing consists of one profile rail

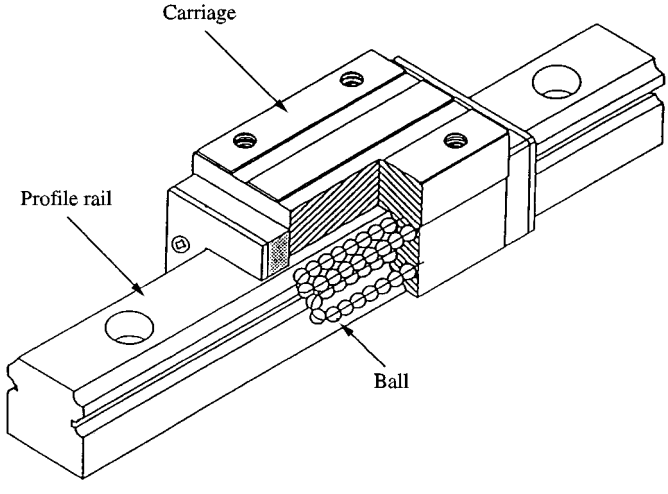

Figure 1. Test linear bearing.

TABLE 1

Test linear bearing specifications

Assembly height	0·040 m
Carriage width	0·048 m
Carriage length	0·079 m
Carriage height	0·033 m
Profile rail width	0·023 m
Profile rail length L	1·000 m
Profile rail height	0·022 m
Ball diameter	$4{\cdot}7625 \times 10^{-3}$
Total number of balls	116
Number of rows	4
Contact angle α	50°
Preload	590 N (light preloaded bearing) 3600 N (medium preloaded bearing)
Load zone length l_L	0·052 m

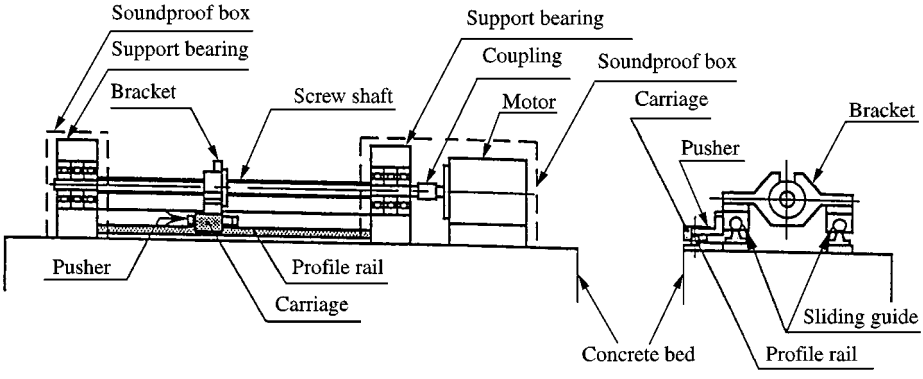

Figure 2. Drive unit.

and one carriage with recirculating balls. Preloads of test linear bearings are light or medium. The preloading for the test linear bearings was made by inserting balls slightly larger than the ball groove space between the profile rail and the carriage. Table 1 shows the test linear bearing specification. The test linear bearings in this study and those of a previous sound study [10] are identical. All test linear bearings were lubricated with mineral oil (ISO VG56).

2.2. DRIVE UNIT AND MEASURING SYSTEM

Figure 2 shows the drive unit which was developed for sound and vibration measurement of linear motion rolling bearings [11]. The drive unit consists of a motor, a coupling, support bearings, a sliding screw, sliding guides, a pusher, and a concrete bed. The profile rail of a test linear bearing is fixed on the concrete bed by bolts. The carriage of the test linear bearing is driven through a coupling, support bearings, a sliding screw, sliding guides and a pusher from a motor. Therefore, when the motor rotates at a constant speed, the

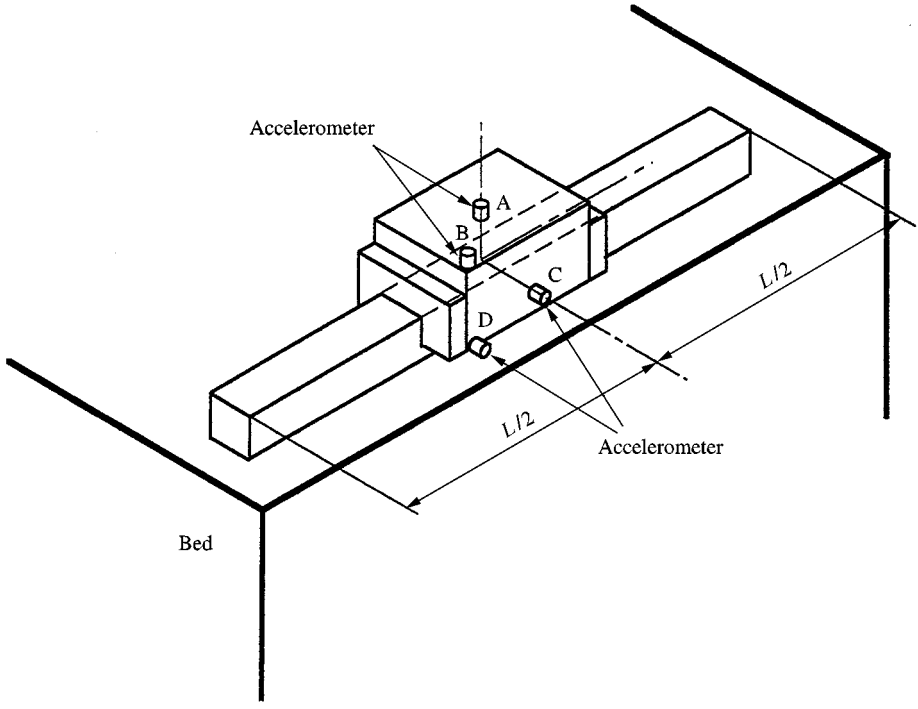

Figure 3. Measurement points of vibration.

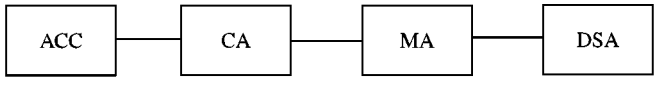

Figure 4. Measuring system for vibration. ACC: Accelerometer, CA: Charge amplifier, MA: Measuring amplifer, DSA: Digital spectrum analyzer.

carriage of the test linear bearing can be driven at a constant linear velocity. Figure 3 shows the measurement points of the vibration. To measure the vibration of the test linear bearing, an accelerometer was attached to the carriage. The measurement points, mounting positions of the accelerometer, were A, B, C and D on the carriage as shown in Figure 3. The vibration of the test linear bearings was detected by the accelerometer when the carriage with a constant linear velocity passed the center in the longitudinal direction of the profile rail. The detected signal of the vibration was amplified by a charge amplifier and a measuring amplifier, and it was examined by a digital spectrum analyzer as shown in Figure 4. In the vibration measurement, the linear velocity of the carriage was varied in 7 steps in the range of 0·333–1·167 m/s.

2.3. CORRECTION FOR AMBIENT VIBRATION

The object vibration in this study is the vibration of the test linear bearing itself. In the vibration measurement, however, the vibration of the drive unit as ambient vibration was

contained in the measured vibration of the test linear bearing. Thus, to accurately evaluate the vibratory velocity level, both overall and at each frequency component of the vibration spectra of the test linear bearing, correction for ambient vibration must be made. In this study, we carried out the correction for the ambient vibration with reference to the correction for the background noise in the sound measurement [12]. The vibratory velocity level of the source alone without ambient vibration is calculated by using the following equation:

$$L_{v1} = L_{v3} - 10 \log \left\{ 1 + \frac{1}{10^{(L_{v3} - L_{v2})/10} - 1} \right\}, \tag{1}$$

where L_{v1} is the vibratory velocity level due to the source alone, L_{v2} is the ambient vibration level, and L_{v3} is the combined level of the source and background. In this study, the vibratory velocity level of both overall and at each frequency component of vibration spectra of the test linear bearing was calculated by equation (1). In addition, we observed that vibratory velocity level below about 100 Hz fluctuated sharply in preliminary experiments. This may be caused by the ball passing vibration [3, 4] which occurred below about 100 Hz. Thus, the overall vibratory velocity level and the vibratory velocity level of the vibration spectra were estimated in the 100–20 000 Hz range. Hereinafter, for convenience of discussion, the overall vibratory velocity level corrected for the background noise in 100–20 000 Hz range is called the overall level.

3. EXPERIMENTAL RESULTS

3.1. OVERALL LEVEL

The overall level of the test linear bearing was examined. The results are presented in Figure 5(a) and (b). The vertical axis is expressed in decibels *re* 1 nm/s. In this figure, the lines denote the least-squares approximation values of the overall level for each measurement point. The gradient values of the lines are listed at the right. It is observed from Figure 5(a) and (b) that the overall levels change with the measurement points, and they are affected by linear velocity and preloads. The overall level of the light preloaded bearing increases about 6·1–8·1 dB as the linear velocity of the carriage increases an octave. The overall level of the medium preloaded bearing increases about 8·2–11·6 dB as the linear velocity increases an octave. Therefore, it is clear that the rate of increase of the overall level to the linear velocity of the medium preloaded bearings is larger than that of the light preloaded bearings.

3.2. VIBRATION SPECTRA

The typical vibration spectra of the test linear bearings are shown in Figure 6(a) and (b). Figures 6(a) and (b) indicates the spectra of the light preloaded bearings and those of the medium preloaded bearing, respectively. The vertical axis is expressed in decibels *re* 1 nm/s. The arrows in the figure show the main peaks in the vibration spectra. The numerical values, which are shown above the arrows, are the frequencies in kHz. It is observed from Figure 6(a) and (b) that the vibration spectra change with the measurement points and they are influenced by the preloads. In other words, the occurrence of the main peaks changes with the measurement points and the preloads. Under the same measurement point, the frequencies of the main peaks of the medium preloaded bearing are higher than those of the light preloaded bearing. In addition, we confirmed that the frequencies of these main peaks

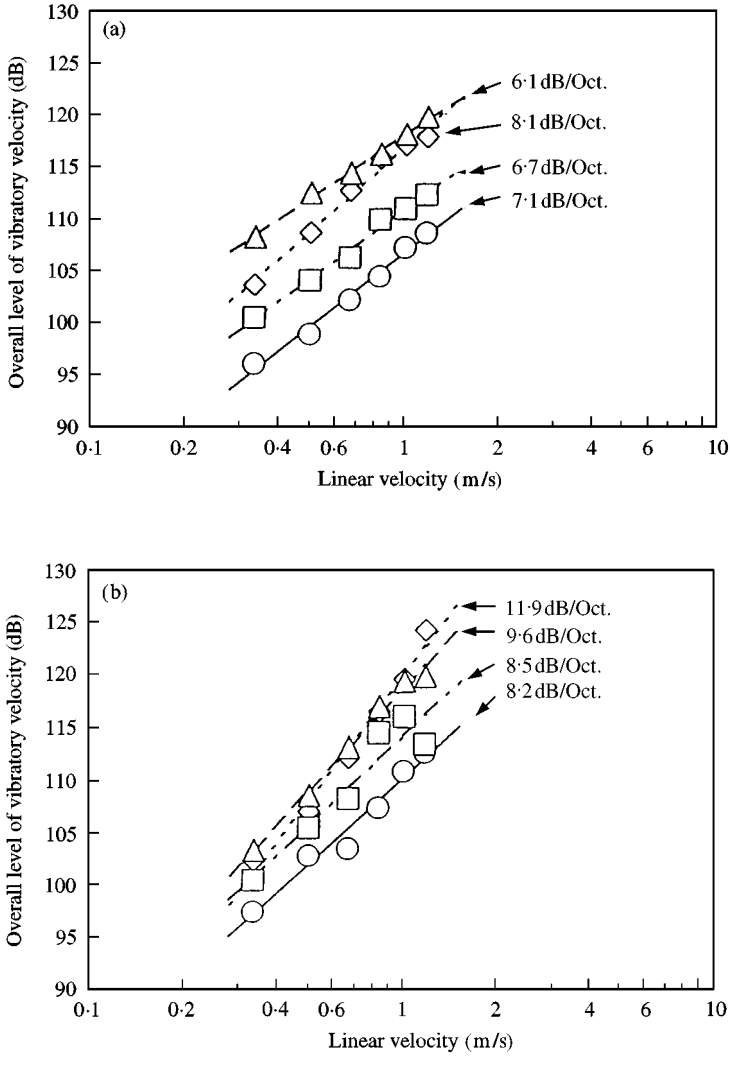

Figure 5. Overall level, linear velocity = 0·833 m/s: (a) light preloaded bearing, —○— measurement point A. —△— measurement point B. —□— measurement point C. —◇— measurement point D. (b) medium preloaded bearing. —○— measurement point A. —△— measurement point B. —□— measurement point C. —◇— measurement point D.

in the vibration spectra of the test linear bearings are not affected significantly by the linear velocity. The average measured frequencies of the main peaks are shown in the left hand column of Table 2.

4. DISCUSSION

4.1. MODAL ANALYSIS

As mentioned in section 3, the frequencies of the main peaks are not affected by the linear velocity. From this fact, it can be assumed that the main peaks are produced by the natural vibrations. In components of LGT recirculating linear ball bearings, the carriage can

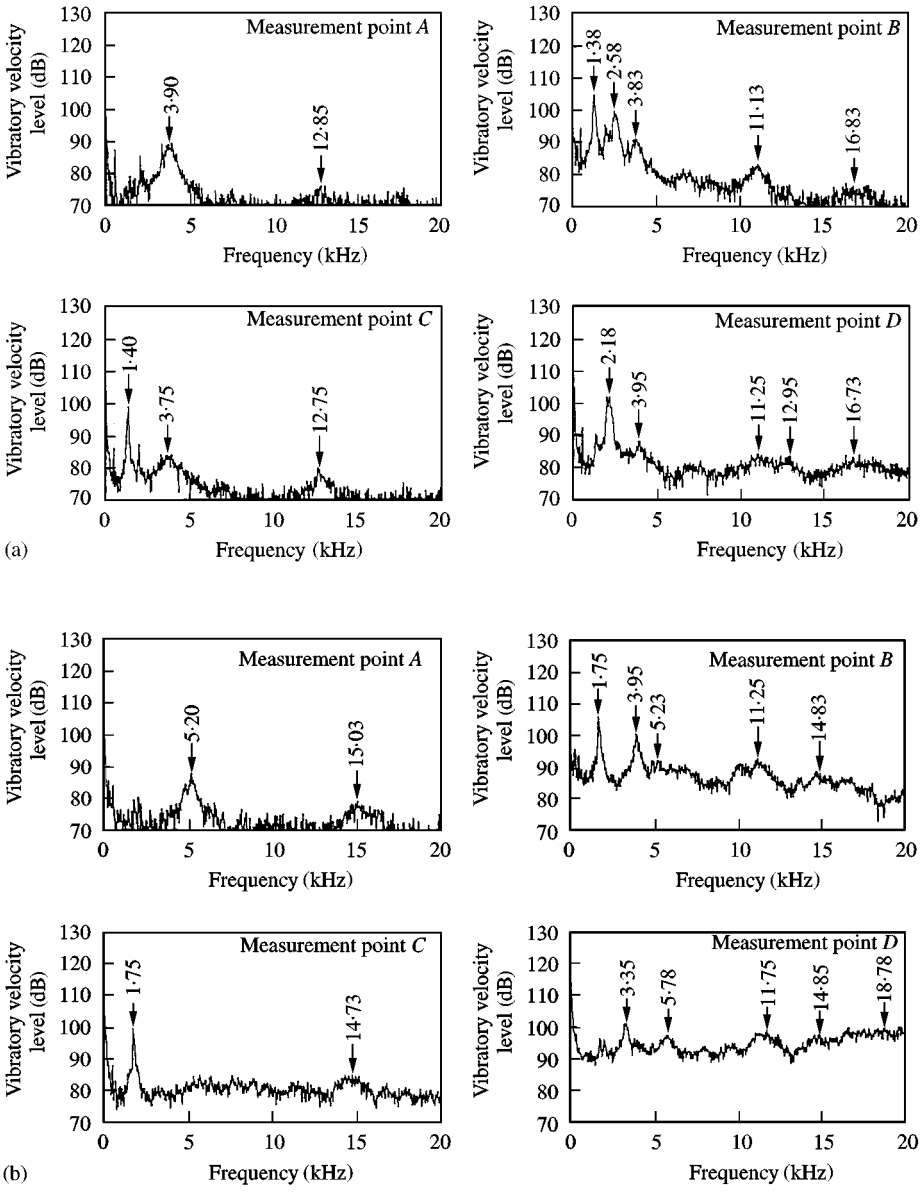

Figure 6. Vibration spectra, linear velocity = 0·833 m/s: (a) light preloaded bearing, (b) medium preloaded bearing.

vibrate easily [6, 9]. We presumed that the main peaks may be caused by the natural vibrations of the carriages of the LGT recirculating linear ball bearings. To examine the relationship between the main peak and the mode of the carriage, an experimental modal analysis was performed. In the modal analysis, the modes of the carriages of the test linear bearings were examined by using two accelerometers and a digital spectrum analyzer as the test linear bearing was driven at a certain linear velocity. Figure 7 shows the modes corresponding to the main peaks. Figure 7(a) and (b) indicates the modes of the light preloaded bearing and those of the medium preloaded bearing, respectively. In this figure,

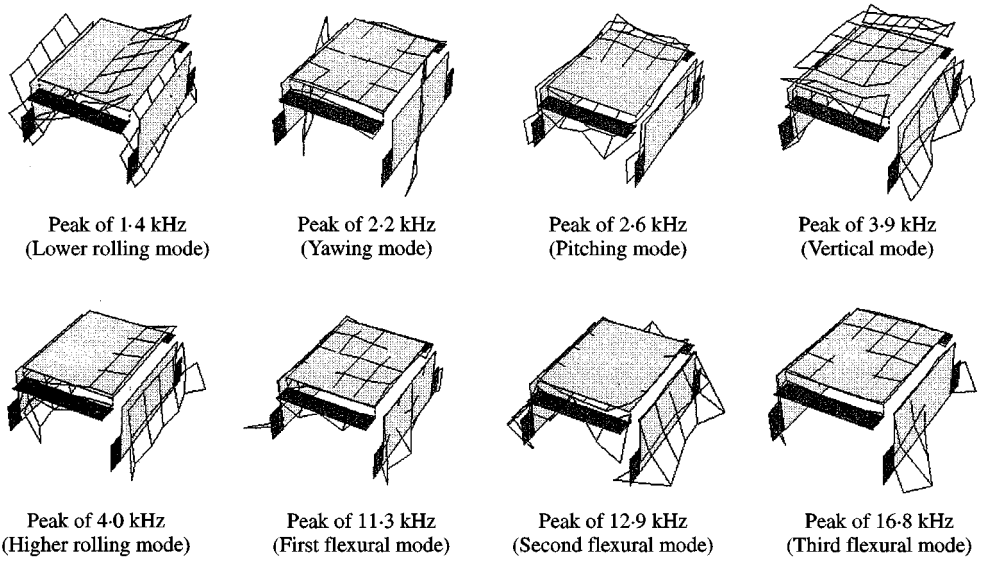

Figure 7. Modes corresponding to main peaks, linear velocity = 0·833 m/s: (a) light preloaded bearing, (b) medium preloaded bearing.

for convenience, the upper face and the side face of the carriage are indicated separately. The shaded faces show the reference faces and the blank faces show the measured mode shape. It is clear that the measured modes are divided roughly into rigid-body modes and the flexural modes of the carriage. The rigid-body modes can be subdivided into the lower rolling mode, the yawing mode, the pitching mode, the vertical mode and the higher rolling mode. The flexural modes can be subdivided into three types. To make a distinction between the three types of flexural modes, we named the first flexural mode, the second flexural mode and the third flexural mode, in the order of increasing frequency. The names of the mode of

TABLE 2

Frequency and mode of test linear bearings: (*a*) *light preloaded bearing*; (*b*) *medium preloaded bearing*

	Measurement		Frequency expression		FEM	
	Frequency (kHz)	Mode	Frequency (kHz)	Mode	Frequency (kHz)	Mode
(a)	1·4	Lower rolling	1·61 (f_{RL})	Lower rolling	1·29	Lower rolling
	2·2	Yawing	1·98 (f_Y)	Yawing	1·93	Yawing
	2·6	Pitching	2·72 (f_P)	Pitching	2·71	Pitching
	3·9	Vertical	3·69 (f_V)	Vertical	3·39	Vertical
	4·0	Higher rolling	3·61 (f_{RH})	Higher rolling	3·52	Higher rolling
	11·3	1st flexural	—	—	8·68	1st flexural
	12·9	2st flexural	—	—	11·15	2st flexural
	16·8	3rd flexural	—	—	13·24	3rd flexural
(b)	1·8	Lower rolling	2·24 (f_{RL})	Lower rolling	1·65	Lower rolling
	3·3	Yawing	2·74 (f_Y)	Yawing	2·55	Yawing
	4·0	Pitching	3·76 (f_P)	Pitching	3·61	Pitching
	5·2	Vertical	5·11 (f_V)	Vertical	4·44	Vertical
	5·8	Higher rolling	5·00 (f_{RH})	Higher rolling	4·77	Higher rolling
	11·6	1st flexural	—	—	8·91	1st flexural
	14·8	2st flexural	—	—	11·94	2st flexural
	18·8	3rd flexural	—	—	13·52	3rd flexural

the carriage are shown in Table 2 by corresponding to the frequency of the main peak. It is clear from Table 2 and Figure 7 that the main peaks have a close relation with the vibration modes of the carriage. Therefore, each main peak is detected easily when the measurement point of the vibration coincides with the loop of the corresponding vibration mode. It is not detected when the measurement point of the vibration coincides with the node. For this reason, the occurrence of the main peaks in the vibration spectra changes with the measurement points.

4.2. ANALYSIS USING FREQUENCY EXPRESSIONS FOR RIGID-BODY NATURAL VIBRATION OF CARRIAGE

4.2.1. *Frequency expressions for rigid-body natural vibration of carriage*

From section 4.1, it can be presumed that the main peaks appearing in the vibration spectra are caused by the natural vibrations of the carriage. Recently, to explain the peaks that appear in the sound spectra of the LGT recirculating linear ball bearing itself, one [10] of the authors considered the vibratory system as shown in Figure 8 and derived the frequency expressions for the rigid-body natural vibration of the carriage. In Figure 8, the origin o of the coordinates $oxyz$ coincides with the position of the center of gravity of the carriage while it does not vibrate. Although the x-axis is not seen in Figure 8, it is parallel to the longitudinal direction of the profile rail. Since the x-axis is also parallel to the driven direction of the carriage, the displacement of the carriage along the x-axis is not considered. Moreover, α is the contact angel, a is the distance from the origin o to the contact point of

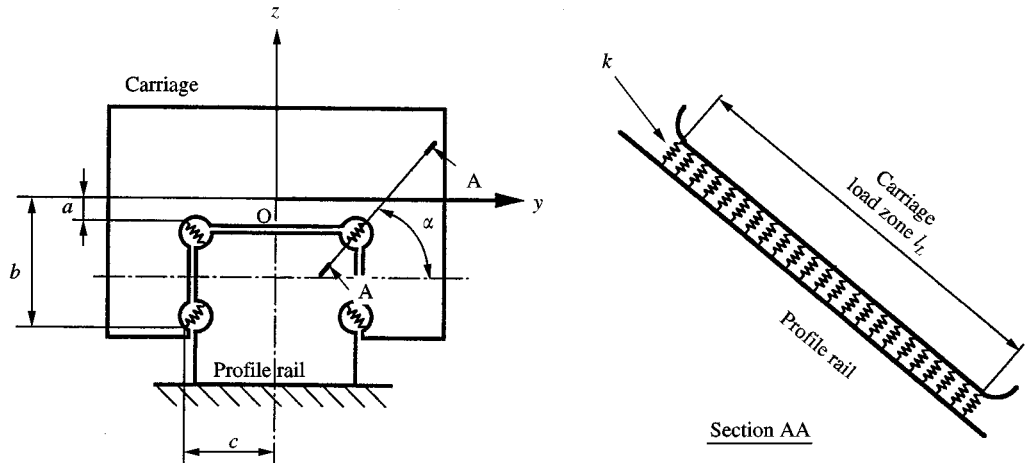

Figure 8. Supporting condition and coordinate of carriage.

the upper circuits of the recirculating balls of the carriage and the distributed normal spring in the direction parallel to the z-axis. b is the distance from the origin o to the contact point of the lower circuits of the recirculating balls of the carriage and the distributed normal spring in the direction parallel to the z-axis. c is the distance from the origin o to the contact point of the carriage and distributed normal spring in the direction parallel to the y-axis. l_L is the length of the load zone in one circuit of the recirculating balls. k is the spring constant per unit length of the distributed normal springs. The spring constant k per unit length of the distributed normal springs can be written as

$$k = \frac{K_V}{4l_L \sin^2\alpha}, \tag{2}$$

where K_V is the vertical spring constant of the LGT recirculating linear ball bearing itself. The frequency expressions for the rigid-body natural vibration of the carriage are as follows: for the frequency f_V of the vertical natural vibration of the carriage.

$$f_V = \frac{\sin\alpha}{\pi}\sqrt{\frac{kl_L}{M}}; \tag{3}$$

for the frequency f_P of the pitching natural vibration of the carriage,

$$f_P = \frac{\sin\alpha}{2\pi}\sqrt{\frac{kl_L^3}{3J_y}}; \tag{4}$$

for the frequency f_Y of the yawing natural vibration of the carriage,

$$f_Y = \frac{\cos\alpha}{2\pi}\sqrt{\frac{kl_L^3}{3J_z}}; \tag{5}$$

for the frequency f_{RL} of the lower rolling natural vibration of the carriage,

$$f_{RL} = \frac{1}{2\pi}\left[\frac{c_3M + c_1J_x - \sqrt{(c_3M + c_1J_x)^2 - 4MJ_x(c_1c_3 + c_2^2)}}{2MJ_x}\right]^{1/2}; \tag{6}$$

TABLE 3

Values of M, J_x, J_y, J_z, a, b, c and k

M	0·465 kg
J_x	$1{\cdot}439 \times 10^{-4}$ kg m^2
J_y	$1{\cdot}937 \times 10^{-4}$ kg m^2
J_z	$2{\cdot}576 \times 10^{-4}$ kg m^2
a	$4{\cdot}18 \times 10^{-3}$ m
b	$13{\cdot}8 \times 10^{-3}$ m
c	$13{\cdot}0 \times 10^{-3}$ m
k	2·05 GPa (light preloaded bearing) 3·93 GPa (medium preloaded bearing)

TABLE 4

Material constants and values of Z'_L, m_b, K_C and K_R for finite element model

	Carriage block	End cap
Young's modulus	206 GPa	3·57 GPa
Poisson's ratio	0·3	0·3
Specific gravity	7·8	1·4
Ball mass	$4{\cdot}41 \times 10^{-4}$ kg	
Spring constants K_C and K_R	$19{\cdot}8 \times 10^6$ N/m (light preloaded bearing) $37{\cdot}2 \times 10^6$ N/m (medium preloaded bearing)	

for the frequency f_{RH} of the higher rolling natural vibration of the carriage,

$$f_{RH} = \frac{1}{2\pi}\left[\frac{c_3M + c_1J_x - \sqrt{(c_3M + c_1J_x)^2 - 4MJ_x(c_1c_3 + c_2^2)}}{2MJ_x}\right]^{1/2}; \tag{7}$$

In equations (2)–(7), M is the mass of the carriage, J_x, J_y and J_z are the moments of inertia about the x-, y- and z-axis, respectively.

4.2.2. *Relationship between main peak with rigid-body mode and rigid-body natural vibration of carriage*

Using the above frequency expressions, we calculated the natural frequencies of the rigid-body natural vibrations of the carriage for the test linear bearing. In the calculation of the natural frequencies, the values of α, l_L are as shown in Table 1 and the values of M, J_x, J_y, J_z, a, b, c and k as listed in Table 3 were used.

The calculated rigid-body natural frequencies of the carriage are shown in the central column of Table 2. It can be seen from Table 2 that the frequencies of the peak with the lower rolling mode, with the yawing mode, with the pitching mode, with the vertical mode and with the higher rolling mode match the calculated frequencies f_{RL}, f_Y, f_P, f_V and f_{RH}, respectively. Thus, it is verified that the main peaks with the rigid-body mode are caused by the lower rolling, the yawing, the pitching, the vertical and the higher rolling natural vibrations of the carriage. In the rigid-body natural vibrations, the existence of the yawing natural vibration and the higher rolling natural vibration of the carriage were not

confirmed experimentally in the sound study [10], but have been verified experimentally and theoretically in this vibration study for the first time.

4.3. ANALYSIS USING FINITE ELEMENT METHOD

4.3.1. *Finite element model*

From section 4.1, it can be presumed that the main peaks with the flexural mode are caused by the flexural natural vibrations of the carriage. Then, to explain the main peaks with the flexural mode, the analysis of the natural vibration of test linear bearings was carried out by the finite element method (FEM). In the analysis, we used the FEM software COSMOS/M. The overall view and the details of the finite element model of the test linear bearing are shown in Figures 9 and 10, respectively. To model the carriage block and the end caps, an eight-node solid element was chosen in COSMOS/M. In the model, the mass m_b of each ball in the load zone. l_L, the spring constant K_C caused by the elastic contact between the carriage and each ball, the spring constant K_R caused by the elastic contact between the profile rail and each ball were considered. To simplify the analysis, we assumed that the ball interval is equal and one ball is located in the center of the load zone as shown in Figure 10. In addition, we assumed that K_C is equal to K_R because the raceway groove radii of the carriage and those of the profile rail in the test linear bearing are identical. Based on these assumptions, K_C and K_R can be expressed as

$$K_C = K_R = 2\frac{l_L k}{Z_L}, \tag{8}$$

where Z'_L is the number of balls in the load zone in one circulation when one ball is located in the center of the load zone. In the analysis using FEM, we used the material constants, Z'_L, m_b, K_C and K_R for test linear bearings as shown in Table 3.

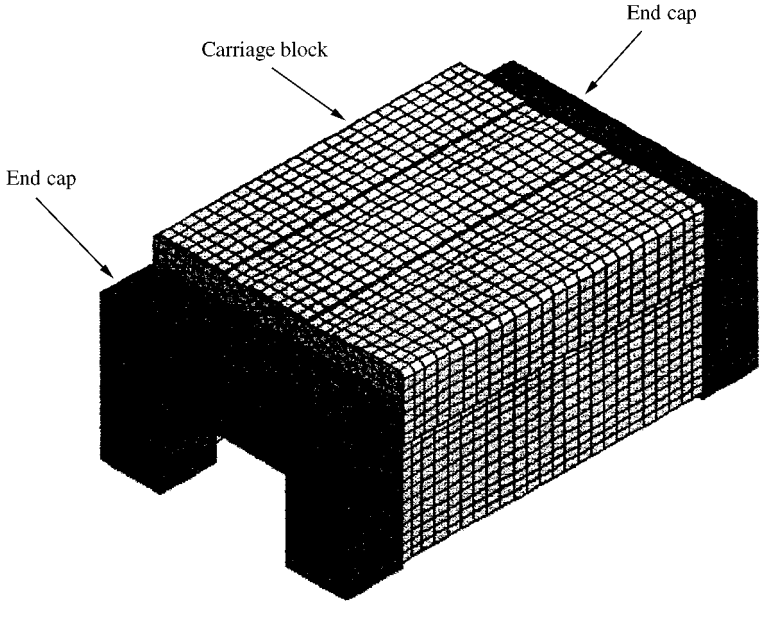

Figure 9. Overall view of finite element model.

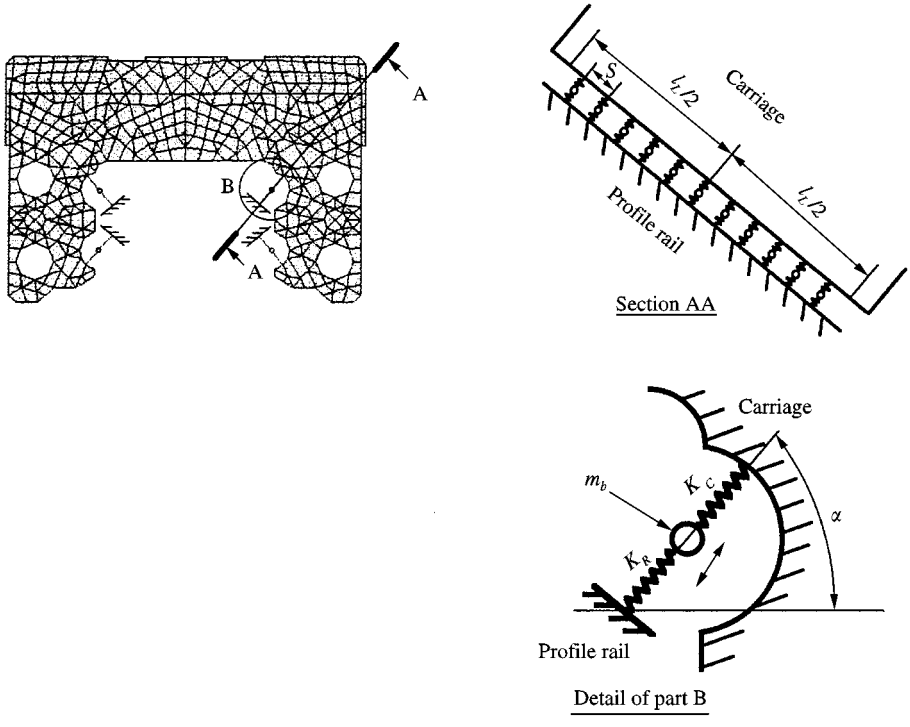

Figure 10. Details of finite element model.

4.3.2. *Results of analysis using the finite element method*

The results of the analysis using FEM on the natural vibration of the carriage are shown in Figure 11(a) and (b). Figure 11(a) and (b) indicates the results of the analysis using FEM of the light preloaded bearing and those of the medium preloaded bearing, respectively. These results are for the 17 652 elements model. In the process of the analysis, we confirmed that each natural frequency calculated by using the number of elements of about 10 000 or more tends to converge to constant values. Moreover, we confirmed that the mode shape is not affected by the number of elements. It is clear from Figure 11 that the flexural natural vibrations of the carriage exist theoretically, in addition to the rigid-body natural vibrations of the carriage. By comparing Figures 7(a), (b) and 11(a), (b), it is clear that the modes of the rigid-natural vibrations and the flexural vibrations of the carriage are almost the same as the measured vibration modes.

To compare the frequency of the main peaks and the natural frequency of the carriage, the results of the analysis using FEM are listed in the right-hand column of Table 2. Although the flexural natural frequencies of the carriage obtained by FEM are lower than those of the main peaks with the flexural mode of the carriage, these are numerically roughly equal. Thus, it is verified that the main peaks with the first, second and third flexural modes of the carriage are caused by the first, second and third flexural natural vibrations of the carriage respectively. Moreover, the rigid-body natural frequencies of the carriage obtained by FEM almost agree with those of the main peaks with the rigid-body mode of the carriage. In addition, the natural frequencies obtained by FEM for the medium preloaded bearing are larger than those for the light preloaded bearing in the same way as

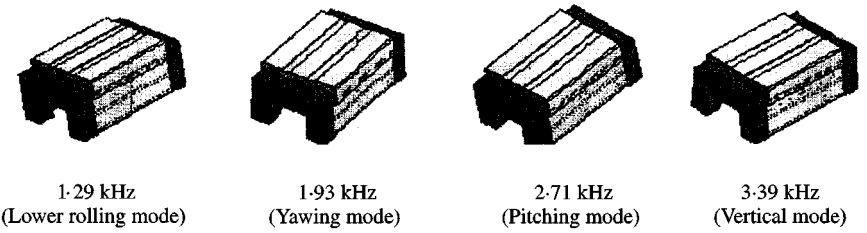

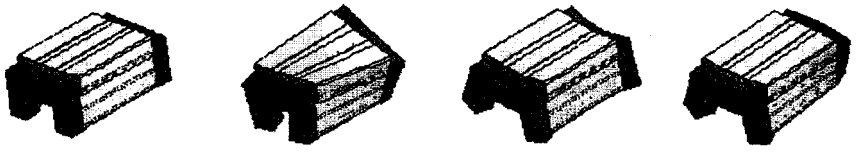

(a)

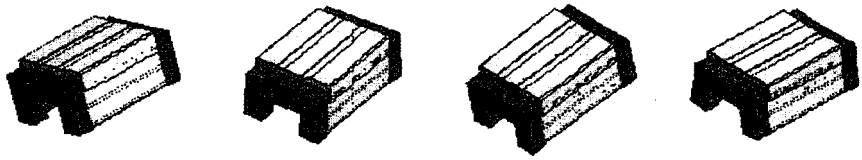

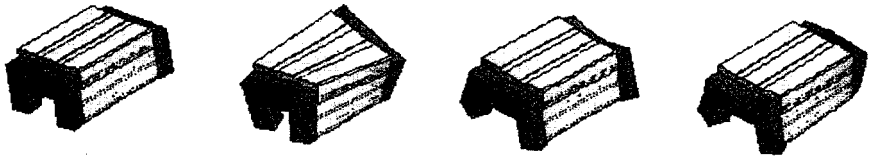

(b)

Figure 11. Analytical results of FEM, 17 652 elements: (a) light preloaded bearing, (b) medium preloaded bearing.

are the frequencies of the corresponding peaks. The reason for this is that the spring constants K_C and K_R of the medium preloaded bearing are larger than those of the light preloaded bearing.

5. CONCLUSIONS

The following conclusions are drawn from the experimental results, the analysis and discussion.

(1) The overall levels of vibratory velocity of the LGT recirculating linear ball bearings change with the measurement point of the vibration, and they are affected by linear velocity and preload.

(2) Several peaks appeared in the vibration spectra of the LGT recirculating linear ball bearings. The occurrence of the main peaks is influenced by the measurement point of the vibration and preload. In addition, the frequencies of the main peaks are not affected significantly by the linear velocity.

(3) The main peaks caused by the following natural vibrations:
   (a) the lower rolling natural vibration of the carriage,
   (b) the yawing natural vibration of the carriage,
   (c) the pitching natural vibration of the carriage,
   (d) the vertical natural vibration of the carriage,
   (e) the higher rolling natural vibration of the carriage,
   (f) the first flexural natural vibration of the carriage.
   (g) the second flexural natural vibration of the carriage,
   (h) the third flexural natural vibration of the carriage.

(4) The frequencies of the rigid-body vibrations of the carriage can be obtained using the frequency expressions f_{RL}, f_Y, f_P, f_V and f_{RH}. Moreover, the frequencies and modes of the rigid-body and the flexural vibrations can be obtained using the finite element method.

REFERENCES

1. H. SCHMITZ and G. LYON 1994 *Machine Design* **66**, 63–65. Picking a better linear bearing.
2. NSK Ltd. 1989 Precision Machine Parts, Pr.No.A1371b.
3. S. KASAI, T. TSUKADA and S. KATO 1987 *NSK Technical Journal* **647**, 39–50. Precision linear guides for machine tools (in Japanese).
4. S. KASAI, T. TSUKADA and S. KATO 1988 *NSK Technical Journal* **649**, 27–36. Recent technical trends of linear guides (in Japanese).
5. S. SHIMIZU 1992 *Journal of JSPE* **58**, 1873–1879. Study on accuracy average effect of linear motion ball guide system (in Japanese).
6. J. YE, N. IIJIMA, F. TASHIRO, S. HAGIWARA and S. YAMADA 1988 *Proceedings of Spring JSPE Meeting*, Vol. **F14**, 199–200. Vibration of linear motion bearing (in Japanese).
7. T. SHIMO 1990 *Machine Design* **62**, 103–106. Linear roller guides.
8. A. GRUNAU and P. GIESE 1991 *Konstruktion* **43**, 111–116. Schwingungsverhalten von Linearwälzführungen für Werkzeugmashinen (in German).
9. M. SCHNEIDER 1991 Statisches und dynamisches Verhalten beim Einsatz linearer Schienenführungen auf Wälzlagerbasis im Werkzeugmaschinenbau. Muchen, Wien: Carl Hanser Verlag (in German).
10. H. OHTA 1999 *Transactions of the ASME, Journal of Tribology* **121**, 678–685. Sound of linear guideway type recirculating linear ball bearings.
11. H. OHTA and T. KAJITA 1996 *An Examined Patent Publication* (*Japan*), *Publication No.* 1996-101059. Drive unit for measurement of vibration and vibration of linear motion rolling bearings.
12. M. FUKUDA 1991 *Handbook of Machine Noise*. Tokyo: Sangyo Tosho Publishing Co., Ltd. (in Japanese).